

On the Energy Spectrum of Cosmogenic Neutrons

A.S. Malgin

Institute for Nuclear Research RAS, Moscow, Russia

E-mail: Malgin@lngs.infn.it

Abstract

The processes of the generation of cosmogenic neutrons (cg-neutrons) underground are considered. The neutrons produced by cosmic-ray muons in their interactions with matter are called cosmogenic. Deep-inelastic πA -collisions of pions in muon-induced hadronic showers are mainly their source at energies above 30 MeV. The characteristics of the energy spectrum for the generation of cg-neutrons have been determined by invoking the additive quark model of deep-inelastic soft processes and the mechanism for the interactions of high-energy nucleons in a nucleus. The three-component shape of the spectrum is explained, and the energy of the “knee” in the spectrum has been found to depend on the mass number A . The peculiarities of deep-inelastic πA -scattering lead to the conclusion that the spectrum of cg-neutrons steepens sharply at energies above 1 GeV. The calculated quantitative characteristics of the spectrum are compared with those obtained in measurements.

Keywords: neutrons, atmospheric muons, underground experiment

A full version was published in *Journal of Experimental and Theoretical Physics*, 2017, Vol. 125, No. 5, pp. 728-740.

1 Introduction

The characteristics of muon-induced cosmogenic (cg) neutrons in various materials deep underground have been actively studied in the last 15 years. These neutrons are among the main sources of the background in the numerous low-background underground experiments that are now underway, with which hopes to detect effects beyond the Standard Model are associated:

hypothetical dark matter particle interactions, neutrinoless double β -decay, and other rare phenomena.

Today it can be stated that one of the main characteristics of the cg-neutron flux, the yield Y_n , has been studied quite well. A relationship of the yield Y_n to the energy losses of ultrarelativistic muons and the mass number of matter A has been established on the basis of experimental data [1]. An analytical expression that allows the yield Y_n and, consequently, the flux and production rate of cg-neutrons to be calculated with a sufficient accuracy for any A at depths greater than 100 m w.e., where the mean energy of the muon flux $\bar{E}_\mu > 40$ GeV, has been derived.

This cannot be said about another important characteristic, the energy spectrum for the generation (the “in-source” spectrum) of cg-neutrons $F^s(T_n)$, where T_n is the neutron kinetic energy. The spectrum $F^s(T_n)$ determines the spectrum $F^{is}(T_n)$ of isolated neutrons (neutrons at the boundary of the semi-infinite layer of material where they are generated), the penetrating power of cg-neutrons, and the set of possible effects produced by them in detectors, shielding materials, and soil.

2 The generation of cosmogenic neutrons

The existing general views of the mechanism for the generation of cg-neutrons by ultrarelativistic muons were shaped within the theory of muon-induced hadronic (h) and electromagnetic (em) showers in matter by invoking the ideas of intranuclear nucleon cascades (INCs) and neutron photoproduction [2],[3].

The basic tenets of these views are:

(a) cg-neutrons at depths greater than 100 m w.e. are generated in any material mainly in showers; the neutrons from $\mu^- A$ -captures dominating at depths up to ~ 100 m w.e. and the photoneutrons produced by a muon through virtual photons constitute a minor fraction in the total number of cg-neutrons;

(b) in any material h -showers make a major contribution to the production of neutrons, despite the much smaller generation cross section of h -showers than that of em -showers, which is explained by the greater multiplicity of neutrons ν_n in h -showers;

(c) the overwhelming majority of h -shower neutrons are produced by the πN -interactions of shower charged pions with nucleons in nuclei; the neu-

trons generated in INCs (*cas*-neutrons), including the πN -scattering recoil neutrons, lie in the entire energy range of cg-neutrons; at energies $T_n > 30$ MeV their mean \overline{T}_n^{cas} is ~ 150 MeV; “evaporative” neutrons (*ev*-neutrons) escaping from remnant nuclei whose number is approximately twice that of *cas*-neutrons and whose energy is $T_n^{ev} < 30$ MeV appear in the last INC phase; a small number of *h*-shower neutrons are produced in $\pi^- A$ -captures and *em*-subshowers initiated by π^0 -decays, these neutrons have energies up to 30 MeV;

(d) the overwhelming majority of *em*-shower neutrons are produced by photons through the giant dipole resonance (GDR), i.e., they are evaporative and have an energy up to 30 MeV; the neutrons from the direct photoeffect (neutron photospallation), the γ -absorption by the deuterium *np*-pair in a nucleus, and the neutrons of *h*-subshowers appearing in emshowers as a result of multiple pion photoproduction can have energies above 30 MeV, but the contribution of the listed channels to the total yield of cg-neutrons is minor;

(e) the spectrum $F^s(T_n)$ is formed by *ev*- and *cas*-neutrons; the number of *ev*-neutrons N_n^{ev} generated in *em*- and *h*-showers exceeds considerably the number of *cas*-neutrons N_n^{cas} ; at $T_n > 30$ MeV the spectrum $F^s(T_n)$ has two segments, flat and steeper, the most common representation of the spectral shape is the dependence $1/T^\alpha$ with different exponents α .

In the absence of a general understanding of the cg-neutron generation mechanism, the above tenets do not give an answer to the following practical questions: (1) whether the dependence $T^{-\alpha}$ corresponds to the cg-neutron generation processes and the exponent α of what quantity can characterize the spectrum $F^s(T_n)$ at $T_n > 30$ MeV before and after the knee; (2) at what energy T_n^{ch} the spectrum changes and what processes cause the knee in the spectrum; (3) whether there can be a “cutoff” in the spectrum and, if so, as a result of what process and at what energy; (4) what fraction in the total number are accounted for by the evaporative neutrons; (5) how the quantities listed in items (1) - (4) depend on the energy \overline{E}_μ and the mass number A of matter.

Establishing the shape of the spectrum $F^s(T_n)$ from experimental data and answering the above questions are complicated by the limited number of measurements and their significant errors. In the time of experimental investigation since 1954 [4] the energy characteristics of cg-neutrons generated by muons with various energies \overline{E}_μ in various materials have been measured in six experiments [5],[6], [7], [8], [9], [10]. The spectrum of isolated neutrons $F^{is}(T_n)$ at energies below 90 MeV was obtained in [5],[6]. The neutron gen-

eration spectrum $F^s(T_n)$ was determined in the last four papers: up to 80 MeV in [7], [10] and up to 400 MeV in [8], [9].

The calculations performed in recent years for various materials using the up-to-date FLUKA and Geant4 software packages [11], [12], [13], [14], [15], [16] (Fig. 1), being in significant disagreement between themselves in spectral shape (and in yield Y_n), do not allow both the characteristics of the spectrum $F^s(T_n)$ for a specific material and their relation to the energy \overline{E}_μ and A to be determined computationally.

3 The production of neutrons in h-showers

The most penetrating neutrons forming the spectrum $F^s(T_n)$ at $T_n > 30$ MeV are produced in h -showers. These showers are initiated by deep-inelastic μA -scattering $\mu A \rightarrow k\pi + mN + (A - m) + \mu'$ (k and m are the multiplicities of the produced pions and nucleons, $m \leq A$) and develop in matter due to the multiplication of pions in deep-inelastic πA -collisions: $\pi A \rightarrow k\pi + mN + (A - m)$. In both μA - and πA -reactions the multiple production of pions is the result of an inelastic collision of the incident particle with one of the intranuclear nucleons. The multiple generation of pions occurs mainly in deep-inelastic soft processes, which make a major contribution to the cross section for the deep-inelastic interaction of hadrons. These processes are characterized by small transverse momenta of generated pions $p_\perp < 1$ GeV/ c , in contrast to the hard ones with $p_\perp > 1$ GeV/ c .

Let us consider the production of neutrons in h -showers in terms of the quark model of strong interactions. In the additive quark model the elastic qq -scattering of two quasi-free valence (structural) quarks (current quarks interact in hard processes) underlies the soft multiple processes. This process can be depicted by a quark diagram (Fig. 2). In this representation of πN -interaction the antiquark of the incident pion \bar{q}_π is elastically scattered by the quark q_N of the target nucleon N . Both quarks acquire momenta sufficient for their escape from the confinements of the interacting hadrons. The breaking of the gluon bond of the scattered antiquark \bar{q}_π to the spectator quark q_π gives rise to virtual $q\bar{q}$ -pairs with their subsequent recombination into a jet of fragmentation pions. The number of recombined $q\bar{q}$ -pairs and, consequently, pions is determined by the energy of the antiquark \bar{q}_π . There is also a leading pion with an energy of about 1/2 of the initial one produced by the spectator quark q_π and the pair antiquark \bar{q} among the fragmentation

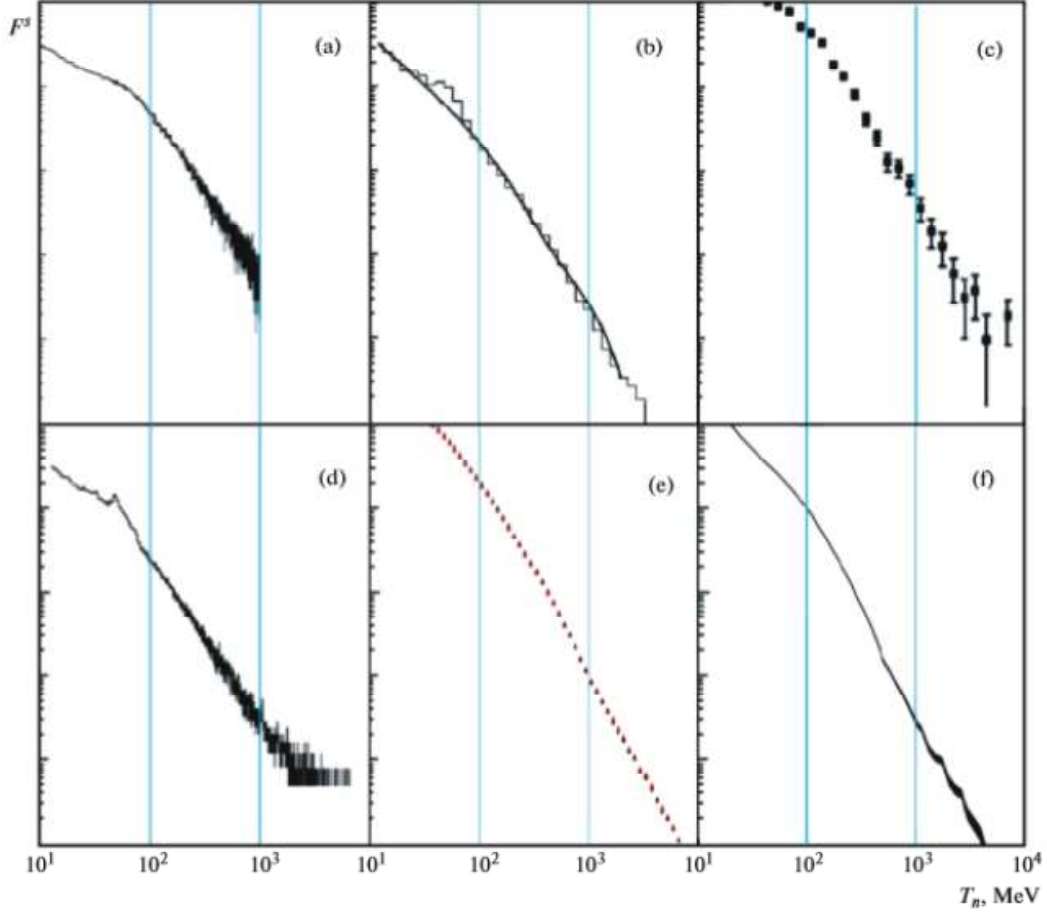


Figure 1: Energy spectra $F^s(T_n)$ for the generation of neutrons by muons of fixed energy E_μ calculated by the Monte Carlo method for various materials: (a) LS, FLUKA, $E_\mu = 285$ GeV [12]; (b) LS, FLUKA and Geant4 (histogram), $E_\mu = 280$ GeV [11]; (c) Pb, FLUKA, $E_\mu = 300$ GeV [14]; (d) LS, Geant4, $E_\mu = 280$ GeV [13]; (e) soil, Geant4, $E_\mu = 275$ GeV [15]; (f) Pb, Geant4, $E_\mu = 260$ GeV [16].

pions. The escape of the quark q_N from the nucleon also gives rise to $q\bar{q}$ -pairs and their recombination into pionization hadrons. The spectator diquark $q_N q_N$ is hadronized (“decolorized”) and turns into a recoil nucleon N_r (r -nucleon).

It is well known from experiments in cosmic rays and on accelerators

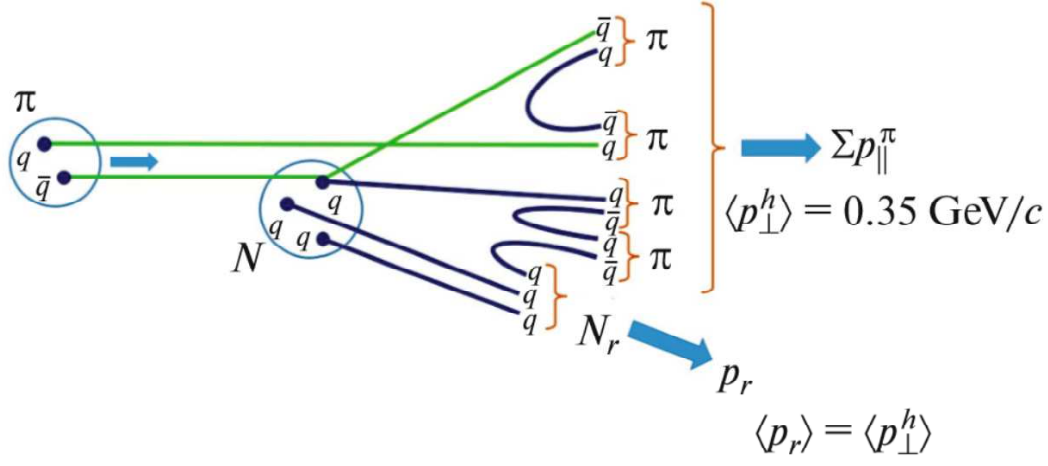


Figure 2: Quark diagram for the collision of valence quarks in deep-inelastic πN -scattering to produce a recoil nucleon N_r in the laboratory frame.

that during the collision of particles with ultrarelativistic energies the pions (hadrons) in the forming jets have an interaction-energy-independent mean transverse momentum $\langle p_{\perp}^h \rangle \approx 0.35 \text{ GeV}/c$. In the QCD theory of strong interactions this quantity corresponds to the scale of gluon vacuum fluctuations with a characteristic nucleon size $\sim 1 \text{ Fm}$ (10^{-13} cm), which is the nucleon confinement size. When gaining an additional momentum (in our case, from \bar{q}_{π}), the quark q_N can reach the confinement boundary (nucleon periphery). Here, the dipole gluon field binding the escaping quark to the diquark $q_N q_N$ is compressed into a string that breaks if the quark has a sufficient momentum. Multiple pion production is a consequence of the breaking.

The gluon string tension is determined by the strong coupling constant. The constant and, consequently, the string tension on the nucleon periphery grow sharply with increasing distance to the escaping quark q_N . The string breaks, on average, at the same tension at a distance $r_q \sim 1 \text{ Fm}$ irrespective of the escaping-quark momentum. As a result, the r -nucleon formed from the diquark $q_N q_N$ gains a momentum p_r directed along the motion of the escaping quark in the nucleus whose mean value must correspond to the string tension at a confinement size $\sim 1 \text{ Fm}$, i.e., $\langle p_r \rangle \approx 0.35 \text{ GeV}/c$, which leads to the equality $\langle p_r \rangle \approx \langle p_{\perp}^h \rangle$. Hence it follows that the mean energy transferred to the r -neutron is independent of the πN -interaction energy and mass number A . The subsequent fate of the r -neutron is determined by its energy and

location in the nucleus. The shower pions produced in πN -collisions escape from the nucleus mostly without any collisions, because their mean free path in nuclear matter, $\bar{\lambda}_{\pi N} \sim 5$ Fm, exceeds the radii of almost all nuclei.

4 The energy spectrum of recoil neutrons $F(\mathbf{E}_r)$

In accordance with the expression $pc = \beta E$ ($E = m_N c^2 + T_N$), the r -nucleon, gaining the momentum $\langle p_r \rangle = 0.35$ GeV/ c , acquires the energy $\bar{\mathbf{E}}_r = 63$ MeV in addition to the energy of its Fermi motion in the nucleus $T_F \approx 30$ MeV. The recoil nucleon can remain in the nucleus, leave the nucleus without any collision, or initiate an INC in an elastic NN -collision. During the INC the r -nucleon energy is fragmented; some of the *cas*-nucleons (including the neutrons) can escape from the nucleus. In an elastic NN -collision the energy is divided between the nucleons, on average, equally unless such a proportion is forbidden by Pauli blocking. Therefore, at the mean energy transfer $\bar{\mathbf{E}}_r = 63$ MeV the *cas*-neutrons escaping from the nucleus have mostly energies in the “evaporative” range approximately up to 30 MeV. Consequently, the neutron energy spectrum at $T_n \geq 30$ MeV is formed by the r -neutrons escaping from nuclei without any collision.

Since the r -neutron is a product of elastic $q_\pi q_N$ -scattering, the spectrum $F(\mathbf{E}_r)$ of q_N -quark energy transfers to the r -neutron must be characterized by the dependence $F(\mathbf{E}_r) \propto 1/\mathbf{E}_r^2$ corresponding to the elastic scattering of two quasi-free point charges. The δ -electrons produced by charged particles during their ionization stopping in matter have the same spectrum. The r -neutron that is capable of producing nuclear particles (p, α, n, t) in inelastic nA -reactions after its escape from the nucleus corresponds to the definition of a δ -particle. The r -neutron in the nucleus must gain the minimum energy $\mathbf{E}_r^{min} = \varepsilon_b + \varepsilon_{th} = 15$ MeV to be transformed into a δ -neutron, because its binding energy in the nucleus is $\varepsilon_b \approx 8$ MeV and the threshold of inelastic nA -reactions is $\varepsilon_{th} \approx 7$ MeV [17].

The existence of minimum energy transfer \mathbf{E}_r^{min} at a given mean energy $\bar{\mathbf{E}}_r$ of the spectrum of a known shape, $F(\mathbf{E}_r) = \text{const} \mathbf{E}_r^{-2}$, points to the existence of a limiting r -neutron energy \mathbf{E}_r^{max} . Its value can be found using the definition of the mean:

$$\bar{\mathbf{E}}_r = \frac{\int_{\mathbf{E}_r^{min}}^{\mathbf{E}_r^{max}} \mathbf{E}_r F(\mathbf{E}_r) d\mathbf{E}_r}{\int_{\mathbf{E}_r^{min}}^{\mathbf{E}_r^{max}} F(\mathbf{E}_r) d\mathbf{E}_r} = \frac{\mathbf{E}_r^{min} \mathbf{E}_r^{max} \ln(\mathbf{E}_r^{max} / \mathbf{E}_r^{min})}{\mathbf{E}_r^{max} - \mathbf{E}_r^{min}} \quad (1)$$

At $\mathbf{E}_r^{max} \gg \mathbf{E}_r^{min}$ this expression takes the form $\bar{\mathbf{E}}_r \approx \mathbf{E}_r^{min} \ln(\mathbf{E}_r^{max} / \mathbf{E}_r^{min})$; substituting $\bar{\mathbf{E}}_r = 63$ MeV and $\mathbf{E}_r^{min} = 15$ MeV here yields $\mathbf{E}_r^{max} \approx 1$ GeV. \mathbf{E}_r^{max} is the maximum energy transfer to the r -nucleon in deepinelastic soft πN -scattering that is determined by the tension energy of the gluon string between the valence quark q_N and the diquark $q_N q_N$ before its breaking.

Note that the ‘‘transverse’’ energy of 1 GeV corresponding to the momentum $p_\perp = 2$ GeV/ c is at the boundary of the region where the hard processes involving current quarks begin to contribute to the total deep-inelastic scattering cross section.

As follows from Eq. (1), at fixed $\bar{\mathbf{E}}_r$ the energy \mathbf{E}_r^{max} depends strongly on \mathbf{E}_r^{min} . Despite being physically justified, its choice contains certain arbitrariness that admits a deviation of about 50% from the chosen value. Thus, at $\mathbf{E}_r^{min} = 11.5$ MeV and $\mathbf{E}_r^{min} = 18.5$ MeV for \mathbf{E}_r^{max} we obtain 2.8 and 0.6 GeV, respectively. Assuming that the range of transverse energies below 1 GeV includes the overwhelming majority of soft processes, below we adopt $\mathbf{E}_r^{max} = 1$ GeV.

5 The spectrum of δ -neutrons

The spectrum of δ -neutrons $F(T_\delta)$ is formed by the r -neutrons (Fig. 2) that escaped from the nuclei without any collisions (T_δ is the neutron energy outside the nucleus). The energy spectrum of r -neutrons before their escape from the nucleus $F(T_r)$ is specified by the spectrum of energy transfers $F(\mathbf{E}_r)$ including the Fermi energy T_F : $F(T_r) = F(\mathbf{E}_r + T_F)$. When escaping freely from the nucleus, the r -neutron loses the energy T_F and the binding energy $\varepsilon_b \approx 8$ MeV; consequently, $T_\delta^{min} = \mathbf{E}_r^{min} - \varepsilon_b \approx 7$ MeV and $T_\delta^{max} = \mathbf{E}_r^{max} - \varepsilon_b \approx 10^3$ MeV. The effect of limiting nuclear fragmentation, i.e., the number of secondary slow particles and the mean energy of δ -nucleons do not depend on the primary particle energy if it exceeds ~ 5 GeV [18], [19], detected in photoemulsion experiments points to a ‘‘cutoff’’ of the δ -neutron spectrum.

The existence of maximum energy T_δ^{max} based on the model of deepinelastic soft πN -scattering does not mean a complete cutoff of the δ -neutron

spectrum. There are processes that give rise to δ -neutrons with an energy above 1 GeV. These primarily include the elastic πN -scattering in the range of pion energies $E_\pi > 10$ GeV, where neutrons with an energy $T_\delta > 1$ GeV can be produced. The elastic πN -scattering cross section, $\sigma_{\pi N}^{el} \approx 4$ mb, accounts for no more than 20% of the inelastic one, $\sigma_{\pi N}^{in} \approx 20$ mb. Other processes, such as the neutron stripping by real and virtual high-energy photons and deep-inelastic hard πN -scattering, make a contribution less than 2% of the elastic scattering contribution. Thus, by the cutoff of the δ -neutron spectrum at an energy of ~ 1 GeV we mean its sharp steepening.

The probability of the escape of an r -neutron from nuclei without any collision is determined by the place of its appearance in the nucleus (the πN -interaction point) and the mean free path in the nuclear matter $\bar{\lambda}_r$. The distribution of πN -collisions in the nucleus does not change with shower pion energy but is related to the mass number A . The cross section for deep-inelastic pion scattering by a free nucleon in the energy range 5 – 100 GeV is virtually constant: $\sigma_{\pi N} \approx 20$ mb [20]. The effective πN -scattering cross section in the nucleus, $\sigma_{\pi N}^{eff}$, is smaller due to the nucleon shadowing: $\sigma_{\pi N}^{eff} = \sigma_{\pi N} A^{\alpha-1}$, where $\alpha = 0.75$ is the shadowing parameter [21]. Thus, the mean free path of a high-energy pion in nuclear matter, $\bar{\lambda}_{\pi N}$, is expressed by the dependence $\bar{\lambda}_{\pi N} = (\sigma_{\pi N}^{eff} \bar{n}_\chi)^{-1}$ cm, where \bar{n}_χ is the average nucleon concentration on the pion path χ . The pion, on average, crosses a nucleus of radius R along the chord $\bar{\chi} = 4R/3 = [4(1.3A^{1/3})/3]$ Fm = $1.73A^{1/3}$ Fm located at a distance of about $3R/4$ from the nuclear center. The distribution of nucleon concentration along the nuclear radius is described by the expression

$$n(R) = n_0 \left(1 + \exp \frac{R - R_0}{\Delta} \right), \quad (2)$$

where $n_0 = \text{const}$ is the nucleon concentration in the core of the nucleus, which is related to the mean nucleon concentration in the nucleus, \bar{n} , by the relation $n_0 = 1.9 \bar{n}$; $R_0 = 1.08A^{1/3}$ Fm is the distance from the nuclear center to the region with the number density $n_0/2$; $\Delta \approx 0.55$ Fm is the rate of decrease in concentration n on the nucleus periphery. The concentration \bar{n}_χ is related to n_0 and the mean concentration of nucleons in the nucleus, $\bar{n} = 10^{38} \text{ cm}^{-3}$: $\bar{n}_\chi \approx 0.4 n_0 \approx 0.76 \bar{n}$. Substituting \bar{n}_χ and $\sigma_{\pi N}^{eff}$ into the expression for $\bar{\lambda}_{\pi N}$, we obtain $\bar{\lambda}_{\pi N} \approx 6.58 A^{1/4}$ Fm. The integral probability of a πN -collision, $P_{\pi N}$, on a path length $\bar{\chi}$ is determined by the ratio $\bar{\chi}/\bar{\lambda}_{\pi N}$:

$$P_{\pi N} = 1 - \exp(-\bar{\chi}/\bar{\lambda}_{\pi N}).$$

The quantity $\bar{\chi}/\bar{\lambda}_{\pi N}$ is weakly related to A ($\bar{\chi}/\bar{\lambda}_{\pi N} = 0.263 A^{1/12}$); it can be assumed to be a constant, $\bar{\chi}/\bar{\lambda}_{\pi N} \approx 0.368$ at $A^{1/12} \approx 1.4$. In that case, $P_{\pi N}$ is also a constant: $P_{\pi N} = 0.308$.

We will consider the median length l_m in the distribution of πN -collisions along the chord $\bar{\chi}$ to be the effective distance from the entrance point of the pion into the nucleus to its collision with the nucleon. It is determined from the equation $0.5 P_{\pi N} = 1 - \exp(-l_m/\bar{\lambda}_{\pi N})$:

$$l_m = -\bar{\lambda}_{\pi N} \ln(1 - 0.5P_{\pi N}) = 1.10A^{1/4} \text{Fm}. \quad (3)$$

Consequently, the r -neutron appears at the distance $\bar{l}_r = \bar{\chi} - l_m = 1.32 A^{1/4}$ Fm along the chord $\bar{\chi}$ before its escape from the nucleus. When the neutron momentum is directed in a cone along the motion of the incident pion, the condition for the escape of neutrons from the nucleus without any collision is that the mean free path of the r -neutron in the nucleus, $\bar{\lambda}_r = (\bar{\sigma}_{nN} \bar{n}_\chi)^{-1}$, exceeds the length \bar{l}_r : $\bar{\lambda}_r \geq \bar{l}_r$. Equating the r -neutron mean free path \bar{l}_r to the length $\bar{\chi} - l_m$ is some approximation, because the recoil neutron is deflected from the trajectory of the pion entering the nucleus under the action of the gluon string tension and its intranuclear motion. The cross section $\bar{\sigma}_{nN}(T_n)$ is an averaged cross section for neutron scattering by nucleons in the nucleus,

$$\bar{\sigma}_{nN} = \frac{(A - Z)\sigma_{nn} + Z\sigma_{np}}{A}, \quad (4)$$

where σ_{nn} and σ_{np} are the effective cross sections for neutron scattering by a free neutron and proton, Z is the number of protons in the nucleus. The dependences of the cross sections σ_{nn} and σ_{np} on energy T_n are presented in Fig. 3. In the range of energies T_n from 30 to ~ 200 MeV σ_{np} is larger than σ_{nn} by a factor of 3 – 1.5. Since $A - Z \approx Z$ for most nuclei, we can assume that in the neutron energy range 30 – 200 MeV $\bar{\sigma}_{nN}$ is virtually independent of the nucleus composition $\bar{\sigma}_{nN} \approx (\sigma_{nn} + \sigma_{np})/2$ and $\bar{\sigma}_{nN} \propto 1/T_n$. At these energies $\overline{\sigma}_{nN}$ can be approximately calculated from the formula $\overline{\sigma}_{nN}(T_n) \approx (6 \times 10^3/T_n)$ mb, where T_n is in megaelectronvolts.

The equality $\bar{\lambda}_r = \bar{l}_r$ and the expressions for $\bar{\lambda}_r$ and \bar{l}_r allow us to determine the critical cross section $\bar{\sigma}_{nN}^{cr} = 100A^{1/4}$ mb and then the corresponding energy T_r^{cr} : $T_r^{cr} = 6 \times 10^3/\bar{\sigma}_{nN}^{cr} \approx 60A^{1/4}$ MeV. This is the threshold value for a free r -neutron escape from the nucleus. The energy $T_\delta^{cr} = T_r^{cr} - (T_F + \varepsilon_b) \approx (T_r^{cr} - 40)$ MeV in the spectrum of δ -neutrons $F(T_\delta)$, corresponds

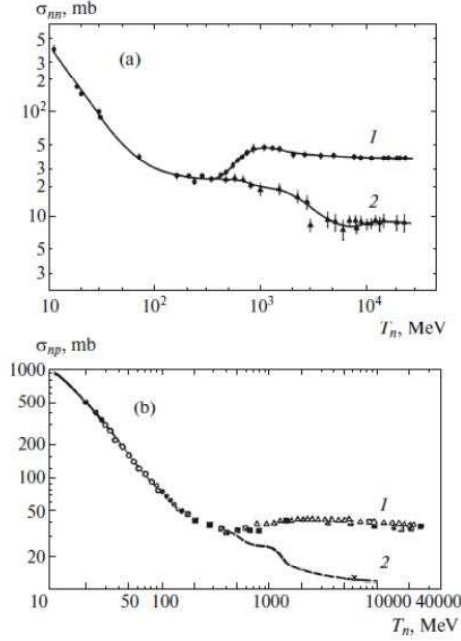


Figure 3: Total (1) and elastic (2) cross sections for neutron-neutron (a) and neutron-proton (b) scattering

to the energy T_r^{cr} in the spectrum $F(T_r)$. Consequently, at δ -neutron energies $T_\delta \geq T_r^{cr}(A)$ the spectrum $F(T_\delta)$ closely follows the shape of the spectrum $F(\mathbf{E}_r) \propto 1/\mathbf{E}_r^2$, i.e., $F(T_\delta) \propto 1/T_\delta^2$.

At $T_r < T_r^{cr}$ the fraction P_δ of r -neutrons freely escaping from the nucleus is determined by the ratio $\bar{\lambda}_r/\bar{l}_r$. Transforming it, we obtain

$$P_\delta \propto \frac{\bar{\lambda}_r}{\bar{l}_r} = \frac{1}{\bar{\sigma}_{nN}(T_r)\bar{n}_\chi\bar{l}_r(A)} \propto T_r A^{-1/4}, \quad (5)$$

because \bar{n}_χ is a constant, $\bar{l}_r \propto A^{1/4}$, and $\bar{\sigma}_{nN} \propto 1/T_r$.

Under the action of the factor P_δ the spectrum $F(T_r)$ in the range ~ 45 MeV $< T_r < T_r^{cr}$ is transformed into the spectrum of δ -neutrons with an energy T_δ from T_δ^{min} to T_r^{cr} :

$$F(T_\delta) \propto F(T_r)P_\delta(T_r) \propto \frac{1}{T_r^2} T_r A^{-1/4} = T_\delta^{-1} A^{-1/4}. \quad (6)$$

Thus, the spectrum of δ -neutrons in any material spans the range from

$T_\delta^{min} \sim 7$ MeV to $T_\delta^{max} \sim 1000$ MeV. The spectrum $F(T_\delta)$ is $1/T_\delta$ in the range from T_δ^{min} to T_δ^{cr} and is described by the law $1/T_\delta^2$ in the range $T_\delta^{cr} - T_\delta^{max}$.

The A dependence of the δ -neutron spectrum $F(T_\delta) \propto A^{-1/4}$ is inverse with respect to the A dependence of the knee energy $T_\delta^{cr} \propto A^{1/4}$. Consequently, the energy T_δ^{cr} increases with A , while the values of the spectrum $F(T_\delta)$ decrease. This is indicative of a decrease in the fraction of δ -neutrons in the total number of cg-neutrons and an increase in the fraction of ev -neutrons. The energy of the knee in the spectrum $F(T_\delta)$ also decreases with decreasing A and then disappears altogether at $A \sim 4$, because all r -neutrons become δ -neutrons. It should be noted that for nuclei with $A < 12$ the expression for T_r^{cr} acquires a large error. This is explained by the absence of a core with a constant concentration n_0 whose size is specified by Eq. (2).

6 Measurements of the cg-neutron production spectrum $F^s(T_\delta)$

The spectrum $F^s(T_\delta)$ of cg-neutrons can be obtained in an experiment whose geometry corresponds to the following requirements:

- (a) the layer of target material where neutrons are produced must be located near the detector at a fixed distance from it, given that the δ -neutrons are directed from top to bottom;
- (b) the target layer must have a fixed thickness of several mean free paths $\lambda_{\pi A}$ but not affecting the shape of the spectrum $F^s(T_\delta)$;
- (c) the presence of a layer of material between the target and the detector must not lead to any deformation of the spectral shape of the neutrons escaping from the target.

In most experiments it is necessary to exclude the detector crossing by a muon and/or a shower, which prevents the energy release of the neutron appearing in the detector from being measured.

The cg-neutron production spectrum $F^s(T_\delta)$ was obtained in the KARMEN [7] and LVD [8] experiments and the Soudan underground laboratory [10]. In the KARMEN experiment the neutrons were generated by muons and showers mainly in a 7000-ton iron shield surrounding a 65 m³ liquid scintillation detector. The crossing by a muon of the planes of the active detector shield, which recorded the time and coordinates of the muon-shower event,

was a trigger for recording neutrons. The events of iron-shield crossing by a muon containing the detector pulses correlated with the muon were selected for the analysis. Since the main goal of the KARMEN experiment was to investigate the νA -cross sections in a beam of accelerator neutrinos, the facility was at a small depth underground. The neutrons from atmospheric muons were studied as a background source in the measurements. The mean energy of the muons passing through the shield corresponded to a depth of ~ 40 m w.e., i.e., it was ~ 15 GeV. Muons of such an energy produce mostly cv -neutrons, because the dominant channels of their generation are the $\mu^- A$ -capture and photoproduction by virtual photons. Nevertheless, recording the temporal, spatial, and energy characteristics of scintillation detector pulses allowed one to establish the energy releases of δ -neutrons escaping from the iron shield and then to determine the shape of the spectrum of “visible” energy releases in the energy range 20 – 80 MeV. The authors of [7] fitted the spectrum of recorded cg -neutron energy releases $F(\varepsilon_{vis})$ by the law $exp(-\varepsilon_{vis}/\varepsilon_0)$, where $\varepsilon_0 \approx 42$ MeV (Fig. 4). As follows from the graph, in the range 30 – 80 MeV being discussed 38 and 19 of the 59 experimental data points lie, respectively, above and below the straight line representing the law $exp(-\varepsilon_{vis}/42)$; two points visually agree with the fit. The discrepancy between the experiment and the dependence $exp(-\varepsilon_{vis}/42)$ is most pronounced in the tail of the spectrum: at a measurement uncertainty of about 35% in the energy range 60 – 80 MeV 17 of the 20 data points lie above the straight line. The exponential with $\varepsilon_0 = 57.8 \pm 9.4$ is the best fit to the KARMEN data in the range 20 – 80 MeV. The significant error in ε_0 is related to the determination of count rates from the graph in Fig. 4. Taking this fact into account, we assume below that $\varepsilon_0 \sim 60$ MeV. This value is supported by the result of the Soudan experiment [10] described below.

The relationship between the dependences $F(\varepsilon_{vis}) \propto exp(-\varepsilon_{vis}/60)$ and $F(\varepsilon_{vis}^\delta)$ is shown in Fig. 5. The curve $F(\varepsilon_{vis}^\delta)$ represents the dependence $N(T_\delta) \propto T_\delta^{-1}$, where the energy T_δ was recalculated to the visible energy release ε_{vis}^δ using the quenching function $q(T_\delta) = \varepsilon_{vis}^\delta/T_\delta$ obtained for an organic liquid scintillator (LS) with an approximate composition $C_{10}H_{20}$ in [22]. Here, the neutron was assumed to transfer all its energy T_δ to one recoil proton, i.e., $T_p = T_\delta$. In reality, the neutron in LS loses its energy in portions in np -scatterings and elastic and inelastic nC -collisions. This assumption affects insignificantly the shape of the curve $F(\varepsilon_{vis}^\delta)$. The curves in Fig. 5 were normalized to the number of events at the energy release $\varepsilon_{vis} = 30$ MeV corresponding to $T_\delta = 47$ MeV. The relative positions of the curves $F(\varepsilon_{vis})$

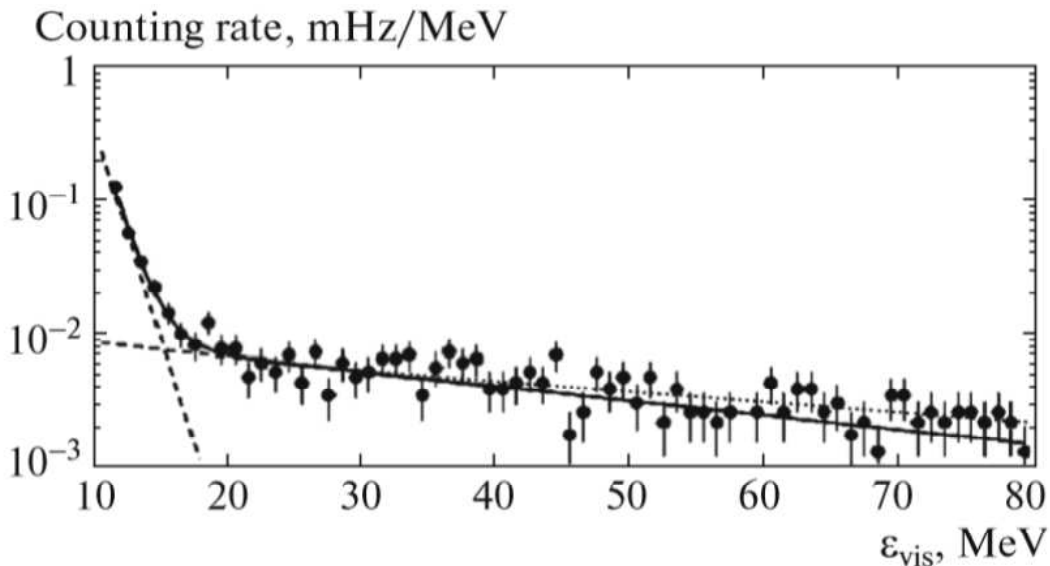


Figure 4: Spectrum of recorded cg-neutron energies in the KARMEN experiment. The solid line is the fit to the data from [7]. The dashed line is the best fit to the data by the law $\exp(\varepsilon_{vis}/60\text{MeV})$ in the range 30 – 80 MeV.

and $F(\varepsilon_{vis}^\delta)$ show that the KARMEN experimental data in the range 30 – 80 MeV can be fitted by the law T_δ^{-1} .

The experiment [10] in an underground laboratory at a depth of 2100 m w.e. ($\bar{E}_\mu \sim 210$ GeV) at the Soudan mine (USA) was aimed at determining the spectrum $F^s(T_\delta)$. The measurements were performed with a cylindrical counter ($\varnothing = 13$ cm, $L = 100$ cm) filled with 12 L of LS. The range of measured energies ε_{vis} is from 4 to 60 MeV. The range was limited from above by the electronics capabilities. The interaction of neutrons in LS was separated from the interactions of electrons, γ -ray photons, and muons by the PMT pulse shape. The low statistics of 24 events in 655 days of measurements underground did not allow definitive conclusions about the shape of the spectrum in the range 30 – 60 MeV to be reached. Of interest are the results obtained by the authors during the calibration measurements on the Earth's surface: the spectrum of neutron energies ε_{vis} in the range 30 – 56 MeV, $\propto \exp(-\varepsilon_{vis}/60\text{MeV})$ (Fig. 6), coincided with the corrected KARMEN spectrum (Fig. 4). Thus, the authors of [10] obtained the spectrum $F^s(T_\delta)$ on the surface. This fact can be explained by the detection of δ -neutrons generated by extensive air shower (EAS) pions in the roof and walls of the

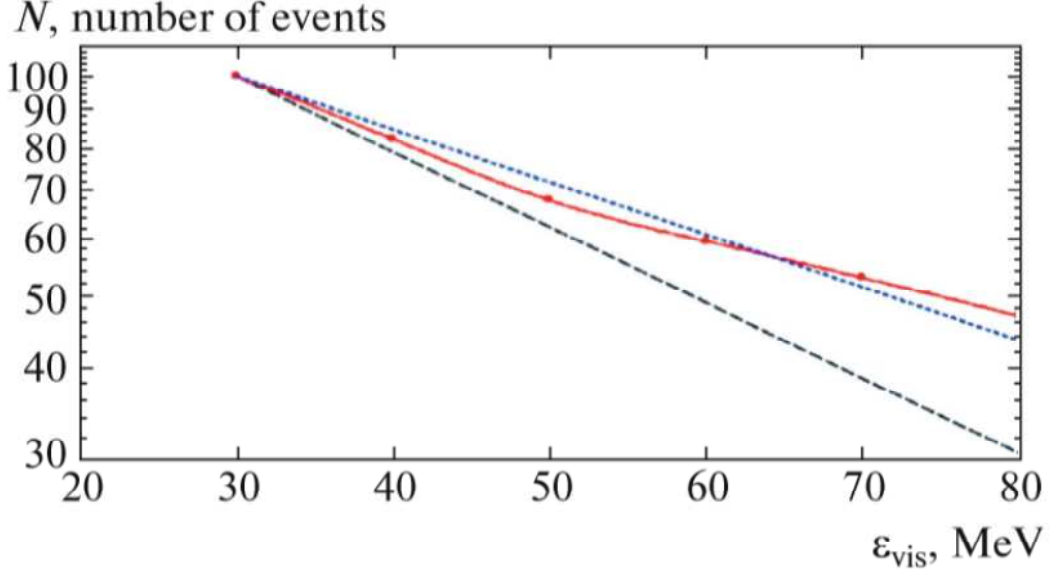


Figure 5: Spectra of recorded cg-neutron energies ε_{vis} in the range 30 – 80 MeV. The dashed line is the fit to the data by the authors of the KARMEN experiment; the dotted line is the fit to the data by the law $exp(-\varepsilon_{vis}/60MeV)$; the solid line is the dependence $1/T_n$ corrected for the quenching. The dependences were normalized at $\varepsilon_{vis} = 30$ MeV.

room in which the measurements were made.

A similar conclusion follows from the measurements of the neutron spectrum in the Gran Sasso National Laboratory at an altitude of 1000 m using a 1.5 m³ scintillator detector [9]. The measured spectrum in the range 30 – 400 MeV with a knee near 90 MeV corresponds to the δ -neutron production spectrum $F^s(T_\delta)$ obtained underground in the LVD experiment [8]. On the surface neutrons with energies above 30 MeV could also be generated by EAS pions in the roof of the experimental room. The similarity of the spectra of neutrons at energies above 30 MeV obtained on the surface and underground has a natural explanation: in both cases, they are generated by h -shower pions in deep-inelastic πA -scattering, whereby the energy characteristics of the produced δ -neutrons do not depend on the pion energy.

The spectrum $F^s(T_\delta)$ of cg-neutrons at a depth of 3650 m w.e. was obtained in the LVD experiment (Fig. 7) [8]. The main goal of the experiment is to detect and investigate the neutrino flux from a gravitational stellar core

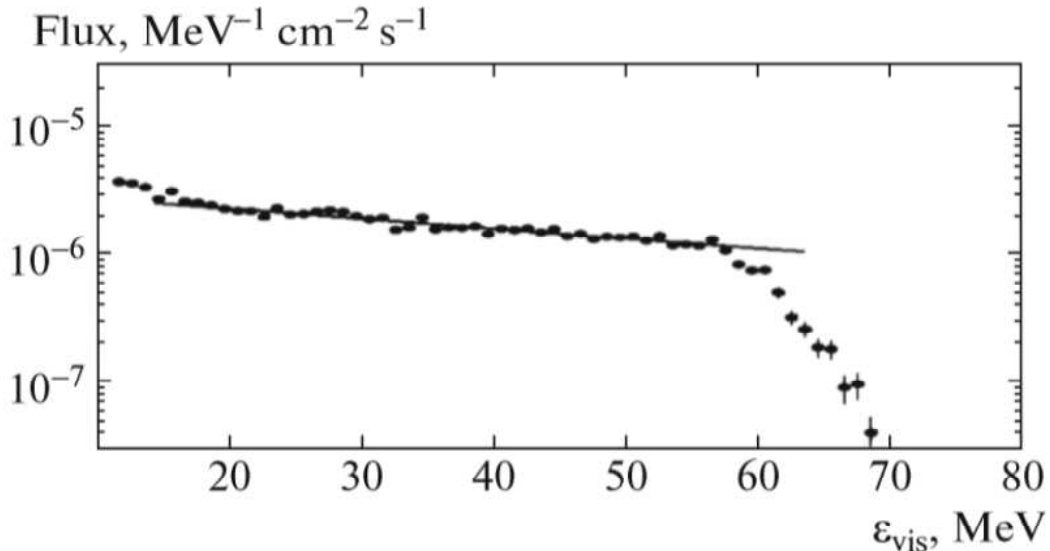


Figure 6: Observed spectrum of cg-neutron energy releases in the Soudan experiment (dots) [10]. The straight line is the dependence $\exp(-\epsilon_{vis}/60 \text{ MeV})$.

collapse. The LVD characteristics also allow the high-energy muons and their interaction products, including the cg-neutrons, to be studied. The rock overburden above the facility determines a mean energy of the muon flux of $280 \pm 18 \text{ GeV}$. LVD consists of three identical $6.2 \times 13.8 \times 10.0 \text{ m}^3$ towers. Each tower contains 280 rectangular 1.5 m^3 counters accommodating 1.2 tons of liquid scintillator each. The counter energy resolution for energy releases above 20 MeV is about 20%, the time resolution is $1 \mu\text{s}$.

Neutrons were generated in the material of the facility composed of LS and iron. Iron is contained in the structural elements of the facility forming a regular cellular structure whose cell is a 1.5 m^3 scintillation counter. The LS and Fe masses are identical, the LS composition is C_kH_{2k} , $k \approx 10$. The spectrum $F^s(T_\delta)$ of neutrons produced by nearly vertical muons in the target column (t-column) of the facility 6.2 m in length, 2.2 m in width, and 7.5 m in height (56 counters with an LS mass of 67 t and the same Fe mass) was reconstructed from the spectrum of “visible” neutron energy releases in 60 scintillation counters of the detecting volume (d-volume) with an LS mass of 72 t [8]. The d-volume is separated from the t-column by a 78 g cm^{-2} LS layer and iron layers with a total thickness of 45 g cm^{-2} contained in the separating half-column (28 counters). The half-column, which incorporates

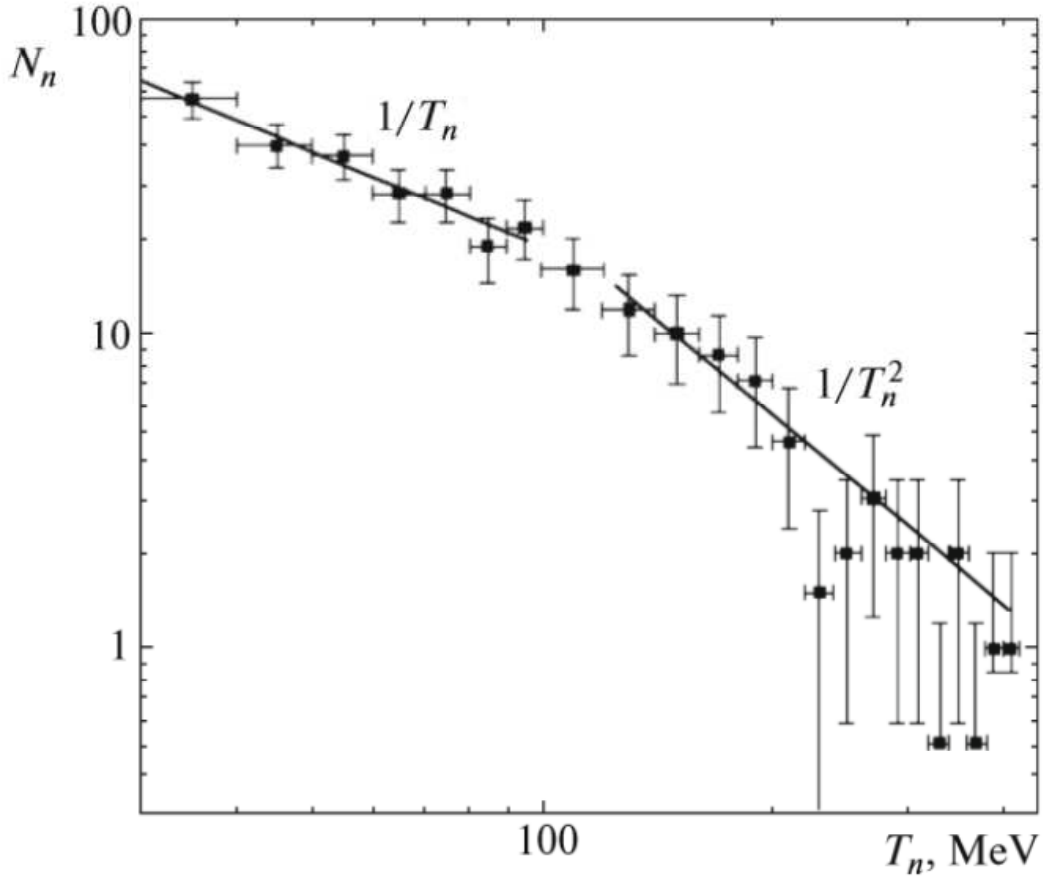


Figure 7: Energy spectrum of cg-neutrons in the LVD experiment [8], N_n is the number of neutrons.

light and heavy materials, efficiently shields the d-volume from the particles of the electromagnetic (γ, e) and hadronic (p, π^\pm) components of the em - and h -showers developing in the t-column. At the same time, the separating half-column with this composition and sizes slightly deforms the shape of the spectrum $F^s(T_\delta)$. This is explained by the following factors. While crossing the half-column, the neutrons with energies $T > 30$ MeV interact mainly with C and Fe nuclei. In elastic nC - and nFe -scatterings the neutrons lose less than 10% of their energy. During an inelastic nA -interaction the δ -neutrons with energies above 30 MeV initiate the development of INCs in the nucleus, which leads to fragmentation of the energy T_δ and practically disappearance of the neutrons with an energy above 30 MeV that experienced inelastic nA -

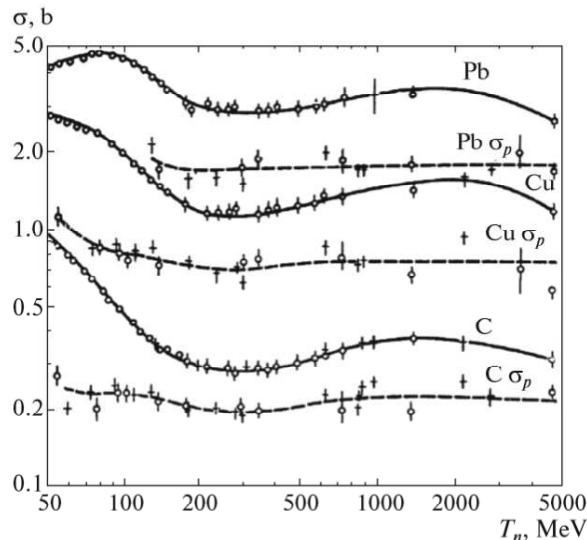


Figure 8: Total and inelastic (σ_p) nA -scattering cross sections for C, Cu, and Pb.

scattering. Since the cross section for this process, while slightly varying, is essentially independent of the incident neutron energy (Fig. 8), the inelastic scattering affects insignificantly the shape of the spectrum $F^s(T_\delta)$.

The np -scattering, as a result of which the neutron loses, on average, half of its energy, could play a prominent role in the processes under consideration. However, since the mean free path of δ -neutrons with $T_\delta > 30$ MeV relative to the np -scattering in LS, $\lambda_{np} > 50$ cm, is comparable to the particle mean path length in LS, 75 cm (the mean length of the counter chord) and since the fraction of np -collisions in LS is about 20%, this process also slightly changes the shape of the δ -neutron spectrum $F^s(T_\delta)$ at the exit from the separating half-column. Monte Carlo simulations [3], [14] also suggest a weak influence of material layer with a thickness up to several mean free paths λ_{nA} on the spectrum shape for neutrons with energies $10 - 10^3$ MeV.

The pulses detected by the d-volume counters in a time interval of 250 ns after a muon event in the target column were attributed to the neutron energy releases. The sought-for spectrum $F^s(T_\delta)$ is formed by the neutrons produced in deep-inelastic πC^- , πFe^- , and πp -interactions whose fractions in the total number of πA -interactions are 48% (πC), 37% (πFe), and 15% (πp). In contrast to the spectrum $F^s(\pi p) \propto 1/T_\delta^{-2}$, the spectra of δ -neutrons in

carbon and iron change their shape at 72 and 124 MeV, respectively. Since the fraction of πp -interactions is small, the measured spectrum $F^s(T_\delta)$ is formed by the neutrons from πC - and πFe -interactions. As a consequence, the spectrum of δ -neutrons is described by the dependence T_δ^{-1} in the energy range from 30 to ~ 70 MeV and by the law T_δ^{-2} above 120 MeV. The LVD data (Fig. 7) are fitted by the law $T_\delta^{-\alpha}$ with $\alpha = 1.11 \pm 0.30$ in the range 30 – 120 MeV and with $\alpha = 2.05 \pm 0.14$ above 120 MeV [8]. The range 70 – 120 MeV is transitional. Since the πC - and πFe -contributions are comparable, the shape of the sought-for spectrum can be assumed to change at an energy ~ 100 MeV, i.e., T_δ^{cr} (LS + Fe) ≈ 100 MeV. Establishing the knee energy T_δ^{cr} allows the characteristics of the spectrum $F^s(T_\delta)$ in the energy range 30 – 400 MeV corresponding to the measurements to be calculated: the mean energy \overline{T}_δ for the entire range 30 – 400 MeV and the mean energies $\overline{T}_\delta^{(1)}$ and $\overline{T}_\delta^{(2)}$ before and after the knee.

Our calculations give $\overline{T}_\delta^{(1)} = 58$ MeV (the range 30 – 100 MeV, $F^s(T_\delta) \propto T_\delta^{-1}$) and $\overline{T}_\delta^{(2)} = 185$ MeV (the range 100 – 400 MeV, $F^s(T_\delta) \propto T_\delta^{-2}$). The spectrum-averaged calculated energy in the range 30 - 400 MeV, \overline{T}_δ , is 107 MeV. For the range of measurements 30 – 1000 MeV the calculated \overline{T}_δ would be 143 MeV. In the experiment (Fig. 7) for total statistics of 371 neutrons (185 and 186 neutrons before and after the knee, respectively) we obtained $\overline{T}_\delta = 104 \pm 6$ MeV, $\overline{T}_\delta^{(1)} = 59 \pm 2$ MeV, and $\overline{T}_\delta^{(2)} = 174 \pm 14$ MeV. It can be seen that the characteristics of the spectrum $F^s(T_\delta)$ calculated for the energy range of cg -neutrons 30 – 400 MeV are consistent with the measurements. The agreement of the calculated characteristics of the spectrum $F^s(T_\delta)$ with the results of the available experiments leads to the conclusion that the model for the production of cosmogenic δ -neutrons considered is efficient.

7 The spectrum of isolated neutrons $F^{is}(T_n)$

In underground experiments the neutron background component produced by cosmogenic isolated neutrons (is -neutrons) is difficult to remove. The neutrons whose appearance is related to the detector neither in time nor spatially are deemed isolated. The neutrons from detector-crossing muons and showers are eliminated by this condition during measurements.

The spectrum of is -neutrons underground $F^{is}(T_n)$ is formed at the rock – experimental chamber boundary. Being equiprobably generated in the

rock volume, the cg -neutrons traverse its various thicknesses, reaching the chamber walls. As a result, the neutron production spectrum $F^s(T_n)$ is transformed into the spectrum $F^{is}(T_n)$. The isolated neutrons in the evaporative region of the spectrum $F^s(T_n)$ at energies $T_n \leq 30$ MeV have an isotropic spatial distribution. Thus, despite the fact that the muon flux and showers are generally directed from top to bottom, the intensity of isolated ev -neutrons escaping from the chamber walls is approximately the same over the entire chamber surface. The attenuation length of ev -neutrons averaged over the rock composition and density ($A = 22$, $Z = 11$, $\rho = 2.65$ g cm $^{-3}$) is $\lambda_n^{is} \approx 25$ g cm $^{-2}$ [23], which determines the small thickness of the rock layer, about 0.3 m, from which the ev -neutrons escape into the chamber. The energy spectrum of isolated ev -neutrons is a composition of the Maxwellian spectra $F^M(T_n) \propto T_n \exp(T_n/T^0)$ with different nuclear temperatures T^0 related to the neutron generation mechanisms in h - and em -showers and the spectrum of δ -neutrons $F^s(T_\delta) \propto 1/T_\delta$ at $T_\delta < 30$ MeV. The mean energy of cosmogenic ev -neutrons is 4 – 7 MeV [2], [24]; at the exit from the rock their energy decreases to 1 – 3 MeV mainly due to their quasi-elastic scattering by rock nuclei. The low energy of cosmogenic ev -neutrons allows the background produced by them to be efficiently suppressed using a detector shield that incorporates active and passive elements.

As has already been noted, cg -neutrons with energies $T_n > 30$ MeV, i.e., δ -neutrons, have the greatest penetrating power. The flux of δ -neutrons underground is characterized by a significant directivity from top to bottom. This is explained, first, by the strong anisotropy of the angular distribution of muons $I_\mu(\theta) \propto \cos^n \theta_\mu$ with an exponent $n \approx 2 - 5$ at a depth of 1000 – 4000 m w.e. under the flat surface, second, by the development of an h -shower along the muon trajectory, and, third, by the escape of δ -neutrons from nuclei in a narrow cone along the motion of the shower pions. The energy dependence of the total nA -interaction cross section in the range 30 – 150 MeV in a standard rock is similar to the energy dependence of the cross section $\sigma_{nN} \propto T_n^{-1}$ (Fig. 8). The mean free path of δ -neutrons λ_δ with energies 30 – 150 MeV lies within the range from 8 to 40 cm. The above peculiarities of cosmogenic particles underground in combination with the δ -neutron isolation condition determine the region from which the neutrons arrive at the detector. It is located above the detector and around its upper part. Apart from the relationship between the detector and chamber surfaces, the shape and sizes of the region depend on the mean free path λ_δ and the angular distribution of δ -neutrons. The number $P_D(T_\delta)$ of is -neutrons

incident on the detector is proportional to the volume of this region $V(T_\delta)$: $P_D(T_\delta) \propto V(T_\delta)$. The longitudinal and transverse sizes of the region are related to the mean free path λ_δ and the angular distribution of δ -neutrons, respectively. In that case, the volume $V(T_\delta)$ can be represented as a cylinder with a height proportional to λ_δ and a cross section proportional to the area $\pi R_\delta^2(\theta_\delta)$:

$$V(T_\delta) \propto \lambda_\delta(T_\delta) R_\delta^2(\theta_\delta).$$

The radius R_δ is related to the ratio

$$p_F^\perp/p_r = \tan\theta_\delta \propto R_\delta,$$

where p_F^\perp is the mean transverse Fermi momentum of the nucleon in the nucleus, p_r is the momentum of the r -neutron, θ_δ is the escape angle of the released δ -neutron from the nucleus relative to the momentum p_r directed along the motion of the shower pion that is slightly deflected from the muon trajectory and the h -shower axis.

Thus, the spectrum of δ -neutrons in the source $F^s(T_\delta)$ under the action of the factor $V(T_\delta)$ is transformed into the spectrum of detected isolated neutrons $F^{is}(T_\delta)$:

$$F^{is}(T_\delta) \propto V(T_\delta) F^s(T_\delta) \propto [\lambda_\delta(T_\delta) \tan^2\theta_\delta] F^s(T_\delta). \quad (7)$$

In the range 30 – 150 MeV the mean free path $\lambda_\delta \propto T_\delta$, because $\sigma_{nA} \propto 1/T_\delta$. Since at these energies $F^s(T_\delta) \propto 1/T_\delta$, $F^{is}(T_\delta) \propto \tan^2\theta_\delta = (p_F^\perp/p_r)^2$. The dependence of $\tan\theta_\delta$ on T_δ obtained at $p_F c = 239$ MeV ($T_F = 30$ MeV) and $T_r = T_\delta + 40$ MeV is presented in Fig. 9. When normalized at $T_\delta = 30$ MeV ($T_r = 70$ MeV, $p_r c = 369$ MeV), it is well fitted by the function $\tan\theta_\delta = 1.8T_\delta^{-0.3}$. Consequently, in the range of isolated δ -neutron energies T_δ^{is} from 30 MeV to the knee (~ 100 MeV) the spectrum $F^{is}(T_\delta)$ underground is

$$F^{is}(T_\delta) \propto \tan^2\theta_\delta \propto T_\delta^{-0.6}. \quad (8)$$

The shape of the spectrum $F^{is}(T_\delta)$ in the range $T_\delta^{cr} \leq T_\delta \leq T_\delta^{max} \approx 1000$ MeV is determined by the quantity $\lambda_\delta(T_\delta)$ and the dependence of $\tan\theta_\delta$ on T_δ . If we assume that in the range 150 – 1000 MeV $\lambda_\delta \approx \text{const}$ (Fig. 8) and $\tan^2\theta_\delta \propto T_\delta^{-0.6}$, then at $T_\delta \approx T_\delta^{cr}$ the spectrum $F^{is}(T_\delta)$ steepens sharply:

$$F^{is}(T_\delta) \propto \lambda_\delta(\tan^2\theta_\delta) F^s(T_\delta) \propto T_\delta^{-0.6} T_\delta^{-2} = T_\delta^{-2.6}. \quad (9)$$

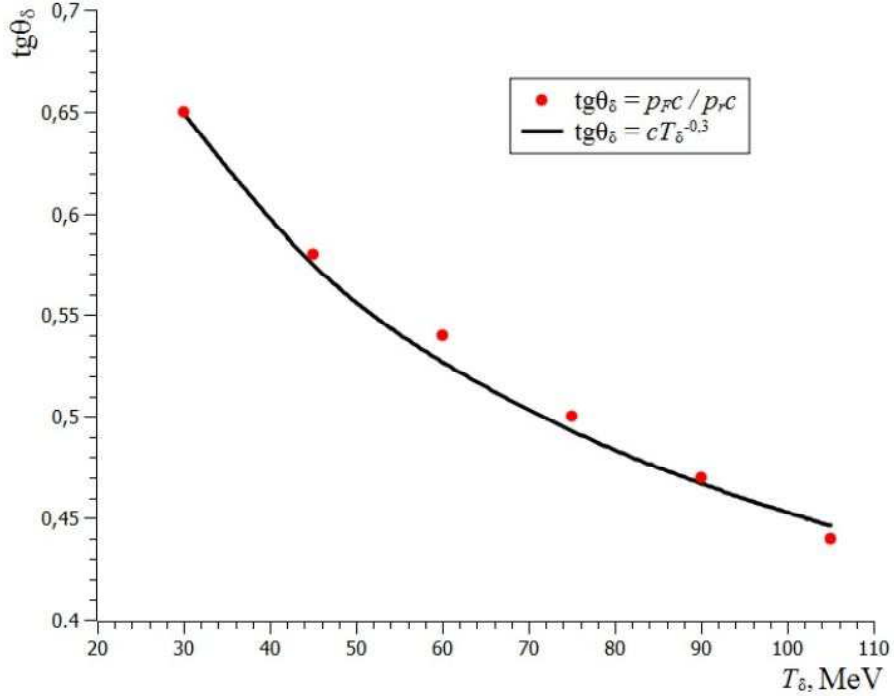


Figure 9: Relationship between the dependence $\tan\theta_\delta = p_F^\perp/p_r$ and the function $T_\delta^{-0.3}$ normalized to $\tan\theta_\delta$ at $T_\delta = 30$ MeV.

The spectrum $F^{is}(T_\delta)$ in the energy range 20 – 90 MeV was measured with the 100-ton cylindrical scintillation detector with approximately equal height and diameter of about 5.5 m. The detector is in a salt mine at a depth of 570 m w.e. [6]. The energy range was determined by the capabilities of the electronics oriented to detect the $\bar{\nu}_e p$ reaction caused by neutrinos from collapsing stellar cores. Neutrons were generated in the salt by a muon flux with a mean energy of ~ 125 GeV. The neutron energy was determined from the energy release of recoil protons in the elastic np -scattering reaction and nC -interaction particles taking into account quenching in a liquid hydrocarbon scintillator. The spectral index was determined with a 20% accuracy (Fig. 10): $F^{is}(T_\delta) \propto T_n^{-0.5 \pm 0.1}$. As can be seen from Fig. 10, the spectrum [6] also agrees satisfactorily with the dependence $T_\delta^{-0.6}$. The spectrum of isolated neutrons generated in h -showers in the rock at a depth of 60 m w.e. by muons at a mean energy of ~ 20 GeV was measured in [5] in the range 10 – 60 MeV (Fig. 10). The neutron energy was also determined from the en-

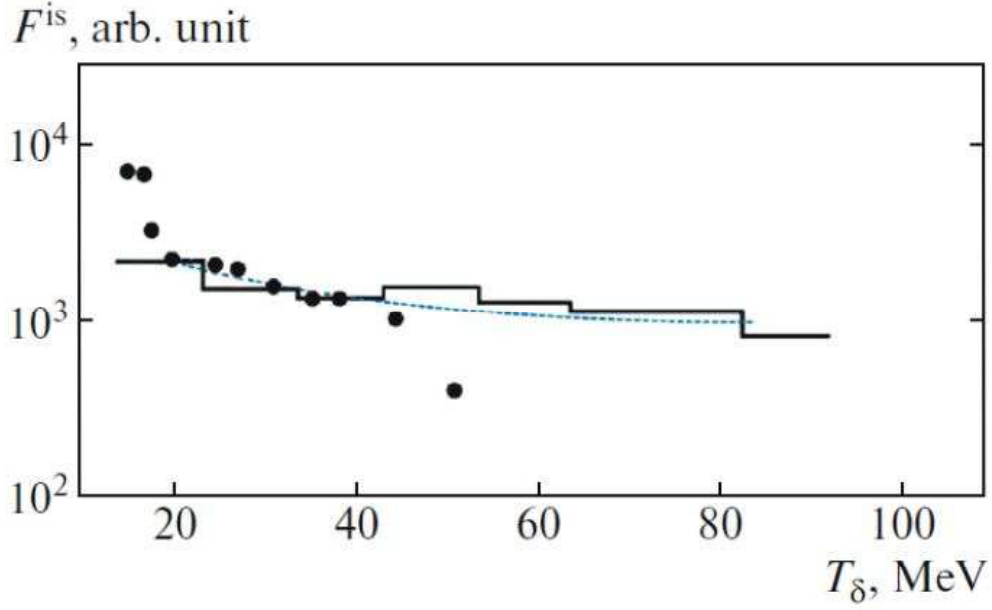


Figure 10: Spectra of *is*-neutrons. The dots are the results from [5], the histogram represents the data from [6], the dashed line indicates the dependence $T_\delta^{-0.6}$. All data were normalized to the value of the histogram at $T_\delta = 20$ MeV.

ergy release of recoil protons in a 3.85-kg cylindrical plastic scintillator with a diameter and height of 17.5 cm. The spectrum [5] in the range from ~ 25 to 40 MeV is slightly steeper than the spectrum [6]. The fall of the spectrum at $T_n > 40$ MeV is explained by the edge effect, which leads to an underestimation of the recoil proton energy. Given the measurement uncertainty, it can be concluded that, being consistent with the experimentally best results of measurements [6], the dependence (8) explains the shape of the spectrum of isolated δ -neutrons with energies from 30 to ~ 100 MeV produced in the rock. Furthermore, the dependence (9) predicts the behavior of the spectrum $F^{is}(T_\delta)$ in the range of energies above ~ 100 MeV, which is not yet provided with measurements.

8 The reaction of δ -neutrons in the total number of cg-neutrons

It is well known from experiments that the number of δ -neutrons N_δ with energies $T_\delta \geq 30$ MeV is approximately half the number of evaporative neutrons N_h^{ev} produced in h -showers [2]. Furthermore, it was found in calculations [11],[25], [26] that the em -shower neutrons N_{em} account for 25 – 40% of the total number of cosmogenic neutrons N_n^{tot} , depending on the material. Assuming that all neutrons N_{em} belong to the evaporative region, we arrive at the equation

$$N_n^{tot} = N_\delta + N_h^{ev} + N_{em} = N_\delta + 2N_\delta + N_{em} = 3N_\delta + \eta N_n^{tot} \quad (10)$$

Hence it follows that $N_\delta = (1 - \eta)N_n^{tot}/3$ and at $\eta = 0.25 - 0.40$

$$N_\delta = (0.20 - 0.25)N_n^{tot} \quad (11)$$

Consequently, the number of δ -neutrons at energies 30 – 1000 MeV and evaporative neutrons (with energies up to 30 MeV) accounts for, respectively, 20 – 25% and 75 – 80% of N_n^{tot} .

9 Conclusions

The cg-neutron production spectrum is explained in terms of the quark model of deep-inelastic πA -scattering. The spectrum is formed by the interactions in nuclei of atoms of the medium. The characteristics of the spectrum (the shape, the mean energy, the knee energy, the mean energies of the spectral ranges) are related to the mechanism for the qq collision of the valance quark of an incident pion with the valance quark of a nucleon in the target nucleus and the passage of the recoil neutron through the nuclear matter.

The spectrum of cg-neutrons occupies the range from zero to ~ 1 GeV and consists of three components. The first component (energies up to 30 MeV) is dominated by evaporative neutrons with a Maxwellian spectrum. The δ -neutrons with a spectrum $1/T_\delta$ present here have virtually no effect on the shape of the resulting spectrum. The mean energy 4 – 7 MeV of neutrons in this spectral range is determined by the value of A and is unrelated to \overline{E}_μ . The neutrons of the first component account for 75 – 80% of the total

number of δ -neutrons, depending on A . The δ -neutrons of deep-inelastic πA -scattering constitute the second and third components spanning the energy range from 30 MeV to ~ 1 GeV. The spectrum of δ -neutrons $F^s(T_\delta)$ has a characteristic shape representable in a logarithmic scale by a straight line with a knee at energy T_δ^{cr} .

The source of δ -neutrons with energies above 30 MeV are h -showers. The neutrons of em -showers and those produced in other processes do not affect the shape of the spectrum. The shape of the spectrum $F^s(T_\delta)$ originates from the energy spectrum of δ -particles $1/T_\delta^2$ that characterizes the elastic scattering of quasi-free valance quarks. The spectrum $F^s(T_\delta)$ is formed by those of the recoil neutrons that escape from the nuclei without collisions. As a result of the interactions of recoil neutrons in the nuclei, the spectrum $1/T_\delta^2$ in the range from 30 MeV to the knee energy T_δ^{cr} takes the shape of the second component $1/T_\delta$. The neutrons of the third component from T_δ^{cr} to ~ 1 GeV have a spectrum $1/T_\delta^2$, because they all escape from the nuclei without collisions. The energy of the knee T_δ^{cr} in the spectrum $F^s(T_\delta)$ depends on A as $T_\delta^{cr} \propto A^{1/4}$; for nuclei with $A \leq 4$ the spectrum $F^s(T_\delta)$ takes a mono shape proportional to T_δ^{-2} , while for $A = 207$ (Pb) the second component of the spectrum proportional to T_δ^{-1} reaches an energy of ~ 190 MeV.

The mean energy of δ -neutrons, $\bar{T}_\delta \sim (120 - 150)$ MeV is weakly related to A and does not depend on the shower pion energy. As a consequence, the shape of the spectrum $F^s(T_\delta)$ and the energy \bar{T}_δ of neutrons generated in the rock remain unchanged with increasing depth and correspondingly rising mean muon energy \bar{E}_μ . For the same reason, the shape of the spectrum $F^s(T_\delta)$ in the atmosphere must closely follow the shape of the δ -neutron spectrum underground.

The energy spectrum of isolated neutrons $F^{is}(T)_\delta$ also has a three-component shape. Here, the mean energy of ev -neutrons of the first component is lower than the mean energy of ev -neutrons of the production spectrum due to the scattering of neutrons by nuclei in the medium. The spectrum of is -neutrons underground $F^{is}(T_\delta)$ at energies above 30 MeV is formed by the δ -neutrons arriving at the detector from the region of their generation without noticeable change in energy and direction. The location of this area relative to the detector and its dimensions are determined by the angular distribution of muons at the depth of observation, the angular distribution of δ -neutrons as they escape from the nuclei, and the mean free path in the rock dependent on their energy. The main factor that determines the shape of the spectrum $F^{is}(T_\delta)$ is the dimensions of the area from which the δ -neutrons reach the

detector. Under the action of this factor the second component of the spectrum $F^s(T_\delta)$ acquires the shape $F^{is}(T_\delta) \propto T_\delta^{-0.6}$, while the third component proportional to T_δ^{-2} is transformed into $T_\delta^{-2.6}$.

One of the revealed important peculiarities is the cutoff of the spectrum at an energy of ~ 1 GeV corresponding to a maximum transverse momentum $p_\perp \sim 2$ GeV/ c in deep-inelastic soft processes. No cutoff has been established so far in measurements, because it is fairly difficult to determine the energy of cg-neutrons in this energy range experimentally. The spectra of cg-neutrons obtained by the Monte Carlo simulation show no sharp change in their shape at energies above 1 GeV (Fig. 1). At the same time, the effect of limiting nuclear fragmentation in a deep-inelastic hadron nucleus interaction and the behavior of the cross section σ_{nN} (Fig. 3) at $T_n \geq 1$ GeV (implying the dominance of pion production in πN -collisions with neutron energy loss both inside and outside the nucleus) point to the existence of a cutoff in the spectrum of cg-neutrons.

The Monte Carlo simulations of the cg-neutron spectrum available to date are inconsistent between themselves and with the measurements. The proposed fits to the data of these simulations by the function $T_n^{-\alpha}$ at $\alpha = \text{const}$ [27], the sum of exponentials $\exp(-aT_n)$, or a combination of these functions [12], [28], [29] do not clarify the cg-neutron spectrum formation mechanism. Monte Carlo calculations do not yet provide simulations of the generation of neutrons by highenergy muons that fit the real one. Knowing the physical processes shaping the spectrum of cg-neutrons allows the Monte Carlo codes needed for the optimization of experiments and the calculation of background effects to be selected and corrected.

Acknowledgements. This work was supported by the Russian Foundation for Basic Research (project No. 15-02-01056a, 18-02-00064a) and the program of investigations of the Presidium of Russian Academy of Sciences High Energy Physics and Neutrino Astrophysics.

References

- [1] N. Yu. Agafonova and A. S. Malgin, Phys. Rev. D 87, 113013 (2013); arXiv:1304.0919
- [2] V. S. Barashenkov and V. D. Toneev, Interaction of High Energy Particles and Atomic Nuclei with Nuclei (Atomizdat, Moscow, 1972) [in Russian].

- [3] A. N. Kalinovskii, N. V. Mokhov, and Yu. P. Nikitin, Penetration of High Energy Particles through the Matter (Energoatomizdat, Moscow, 1985) [in Russian].
- [4] M. Annis, H. C. Wilkins, and J. D. Miller, *Phys. Rev.* 94, 1038 (1954).
- [5] J. C. Barton, in Proceedings of the 19th International Cosmic Ray Conference ICRC, San Diego, 1985, Vol. 8, p. 98.
- [6] F. F. Khalchukov et al., in Proceedings of the 20th International Cosmic Ray Conference ICRC, Moscow, 1987, Vol. 2, p. 266.
- [7] B. Armbruster et al., *Phys. Rev. D* 65, 112001 (2002).
- [8] N. Yu. Agafonova, V. V. Boyarkin, V. L. Dadykin, et al., *Bull. Russ. Acad. Sci.: Phys.* 73, 628 (2009).
- [9] Bonardi et al., in Proceedings of the 31st International Cosmic Ray Conference ICRC, Lodz, 2009, ID icrc05080. <http://icrc2009.uni.lodz.pl/proc/pdf/icrc0580.pdf>.
- [10] C. Zhang and D.-M. Mei, *Phys. Rev. D* 90, 122003 (2014).
- [11] H. M. Araujo, V. A. Kudryavtsev, N. J. C. Spooner, and T. J. Sumner, *Nucl. Instrum. Methods Phys. Res., Sect. A* 545, 398 (2005).
- [12] C. Galbati and J. F. Beacom, *Phys. Rev. C* 72, 025807 (2005).
- [13] O. M. Horn, PhD Thesis (2008).
- [14] V. A. Kudryavtsev, L. Pandola, and V. Tomasello, *Eur. Phys. J. A* 36, 171 (2008).
- [15] R. Persiani, PhD Thesis (Bologna Univ., Italy, 2011).
- [16] L. Reichhart et al., *Astropart. Phys.* 47, 67 (2013).
- [17] V. M. Bychkov, V. N. Manokhin, A. B. Pashchenko, and V. I. Plyaskin, Cross-Sections for Neutron Induced Threshold Reactions, The Handbook (Energoizdat, Moscow, 1982) [in Russian].
- [18] S. Powel, P. Fowler, and D. Perkins, The Study of Elementary Particles by the Photographic Method (Pergamon, New York, 1959).

- [19] Yu. P. Nikitin and I. L. Rozental, High Energy Nuclear Physics (Atomizdat, Moscow, 1980).
- [20] W.-M. Yao et al., J. Phys. G: Nucl. Part. Phys. 33, 1232 (2006).
- [21] Yu. P. Nikitin, I. L. Rozental, and F. M. Sergeev, Sov. Phys. Usp. 20, 1 (1977).
- [22] G. Bruno, JINST 8, T05004 (2013).
- [23] V. I. Ivanov and V. P. Mashkovich, Collection of Problems in Dosymetry and Protection from Ionized Radiations (Atomizdat, Moscow, 1973) [in Russian].
- [24] S. Hayakawa, Cosmic Ray Physics: Nuclear and Astrophysical Aspects (Wiley Interscience, New York, 1969; Mir, Moscow, 1973).
- [25] G. V. Gorshkov, V. A. Zyabkin, and R. M. Yakovlev, Sov. J. Nucl. Phys. 18, 57 (1973).
- [26] O. G. Ryazhskaya, Doctoral (Phys. Math.) Dissertation (Inst. Nucl. Res. RAS, Moscow, 1986).
- [27] Y.-F. Wang, L. Miller, and G. Gratta, Phys. Rev. D 62, 013012 (2000).
- [28] Y.-F. Wang, V. Balic, G. Gratta, A. Fasso, S. Roesler, and A. Ferrari, Phys. Rev. D 64, 013012 (2001).
- [29] D.-M. Mei and A. Hime, Phys. Rev. D 73, 053004 (2006).